




An automated sensitive approach for measuring whole gut transit time

Keeley L. Baker^{1,2} | Michelle Izydorczak¹ | Ruaidhri Jackson³ |
Justus V. Verhagen PhD^{1,2} 

¹The John B. Pierce Laboratory, New Haven, CT, USA

²Department of Neuroscience, Yale School of Medicine, New Haven, CT, USA

³Department of Immunology, Blavatnik Institute, Harvard Medical School, Boston, MA, USA

Correspondence

Justus V. Verhagen, The J. B. Pierce Laboratory, 290 Congress Avenue, New Haven, CT 06519, USA.
Email: jverhagen@jbpierce.org

Funding information

National Institute on Deafness and Other Communication Disorders, Grant/Award Number: R01DC011286 and R01DC014723; National Science Foundation, Grant/Award Number: IOS-1555880

Abstract

Background: Commonly used methods to measure whole gut transit time in rodents have yet to combine high sensitivity, objectivity, and automation. We have developed a novel method using oral gavage of non-toxic fluorescent dye particles and their detection by fluorescence imaging to enable unbiased automated detection of gut transit time simultaneously in 8 cages.

Methods: Naïve mice ($n = 20$) were gavaged with a non-caloric viscous suspension of 4.4% fluorescent dye in 3 groups on 2 occasions. Each group was imaged in 8 cages at 5-minute intervals using blue LEDs for illumination and a Sony full-frame mirrorless camera with a green band-pass emission filter. Custom MATLAB code counted the number of fluorescent boli per cage post hoc and provided graphical and spreadsheet output. Boli counts across a wide range of parameters were compared to blind assessments by an experimenter.

Results: Fluorescent boli were detected with high sensitivity, while unstained boli were readily rejected. All cages showed no fluorescent boli for the first ~20 frames (100 minutes), after which many cages gradually show a rise to 1-6 fluorescent boli. The mean time to first fluorescent bolus in each session was 264 ± 141 and 223 ± 81 minutes post-gavage, with no within subject consistency. There was high correlation between automated scores and that of experimenter ($r = .95 \pm .02$), being robust to parameter changes.

Conclusions and Inferences: This novel approach provides a reliable, automatic, and low-cost method of measuring gastrointestinal transit time in mice.

KEYWORDS

fluorescence, fluorescent imaging, gastrointestinal transit, motility, transit time

2 | INTRODUCTION

Gastrointestinal motility dysregulation has been linked to debilitating diseases such as Crohn's disease, colitis, and irritable bowel disease.¹ The measurement of whole gut transit time in rodents has

provided a pivotal understanding of the complex regulation of gastrointestinal motility that underpins such diseases.

Whole gut transit can be estimated indirectly in terminal experiments, by the measurement of the geometric center of orally administered tracers.^{2,3} Alternatively, steel beads and barium are used in

non-terminal experiments, alongside fluoroscopic video recordings, to record the active transit of the beads over time.⁴ Whole gut transit, however, is most commonly evaluated by the oral administration of a non-absorbable marker such as carmine red and monitoring the first appearance of the stool.⁵⁻¹⁰ This process, however, is time consuming and does not rely on unbiased judgment of the first appearance of the transit marker.

The automation of behavioral monitoring critically provides a greater overall reproducibility of life science research.^{11,12} Experimenter presence or indeed their odor can affect behavioral results^{13,14} and also cause stress for the animals. Stress and subsequent alterations in catecholamine levels also invariably alter GI transit.¹⁵⁻¹⁸ Therefore, the need for automation, free of confounding observer effects to measure gut transit, is paramount. Here, we describe an automated, efficient, and unbiased method of accurately and directly measuring whole gut transit time.

3 | METHODS

3.1 | Animals

Twenty female C57/BL6 (Jax stock #000664) mice were used, randomly separated into three groups (6, 7, and 7 animals, respectively). Mice were housed under standard controlled conditions under an inverted 12-hours light cycle (9.00-21.00). Food and water were available ad libitum. Each group was co-housed in large cages (18 × 10") 1 week prior to experiments. All procedures were performed in accordance with protocols approved by the Pierce IACUC.

3.2 | Gut transit

Mice were fasted for 2 hours after which they were administered 0.3 mL of the fluorescent suspension (0.16 g (fluorescent yellow pigment, "lemon yellow", SolarColorDust, made by Hali Industrial Inc, HLP-8003, <http://www.hali-pigment.com>; 98% amine aldehyde resin, 2% dye; particles size ≤ 3 μm; non-toxic upon ingestion and water insoluble) in 3.6 mL of 0.5% methylcellulose (4000 cP, M0512, 88 000 kD, Sigma-Aldrich) orally by gavage (21-gauge round-tip feeding needle). Mice were placed in individual cages for the duration of the imaging experiment. Experiments lasted 7 hours, and mice were not disturbed.

3.3 | Experimental setup

A white PVC base (38 × 20 × 1/4") covered in black matte card was placed in a fume hood to secure 8 regular mouse cages (11.5 × 7.5"). Clear acrylic sheet was used to cover all cages, with a hole for each cage. Filtered house air was delivered to each cage at 5.9 lpm. Black tape outlined the cage edges on the lid to absorb their fluorescence.

Key Points

- Whole gut transit time measurements in rodents have yet to combine high sensitivity, objectivity, and automation.
- Our new method solves this by using oral gavage of non-toxic fluorescent dye particles and their automated detection by fluorescence imaging.
- Fluorescent boli were detected with high sensitivity, while unstained boli were readily rejected, simultaneously in 8 cages.
- This novel approach improves quality of gastrointestinal transit time measures in mice, can provide bolus counts at any desired interval, and yield quantified motility dynamics.

Thirty-two inches above the base, a PVC bar (42 × 4 × 1/4") was secured via wall-mounted blocks. A centered cylinder (2.5" ID, 1" tall, notched for lens-release button) held the camera above and aimed toward the cages. Five cages were placed side by side against the back wall of the hood and 3 cages front to front (Figure 1A). Visually obscured areas in the most lateral cages were filled with aluminum wedges (4 in total).

3.4 | Lights

Two LED assemblies were positioned to uniformly illuminate the mouse cages with the least imaged reflections. They were positioned 24" apart, 13" above the hood's base using 2 stands (OnStageStandards, LS7720BLT). Each LED assembly contained 4 Luxeonstar SP-03-V4 LED modules (1500 mW output at 350 mA each), each featuring 3 LXML-PR02-A900 Royal-Blue Luxeon Rebel LEDs (440-460 nm), soldered to a SinkPAD-II 20 mm Tri-Star base. They were mounted to a 65-mm OD copper disk, mounted on a fan-cooled aluminum cooling module. The 2 assemblies' 24 LED dies (in 8 modules) were connected as 4 parallel groups of 6 dies in series and fed a 500 mA current, for 125 mA per module and estimated 4300 mW combined light output. Excitation filters (Chroma 490 nm short pass, 70 mm OD) were mounted in custom 3D printed housing.

3.5 | Camera

We used a Sony A7II mirrorless full-frame camera. We mounted a Nikon Nikkor 28 mm F2 Ai-S (iris wide open) via a Nikon F to Sony NEX adaptor (FOTGA, Nikon(G)-NEX). An excitation filter (Semrock, ff01 534/42, 1" OD) was housed in a lens tube (Thorlabs, SM2L05), screwed onto the lens. The camera was powered with an external power supply (CCYC, ECH-168A). An external 4K monitor

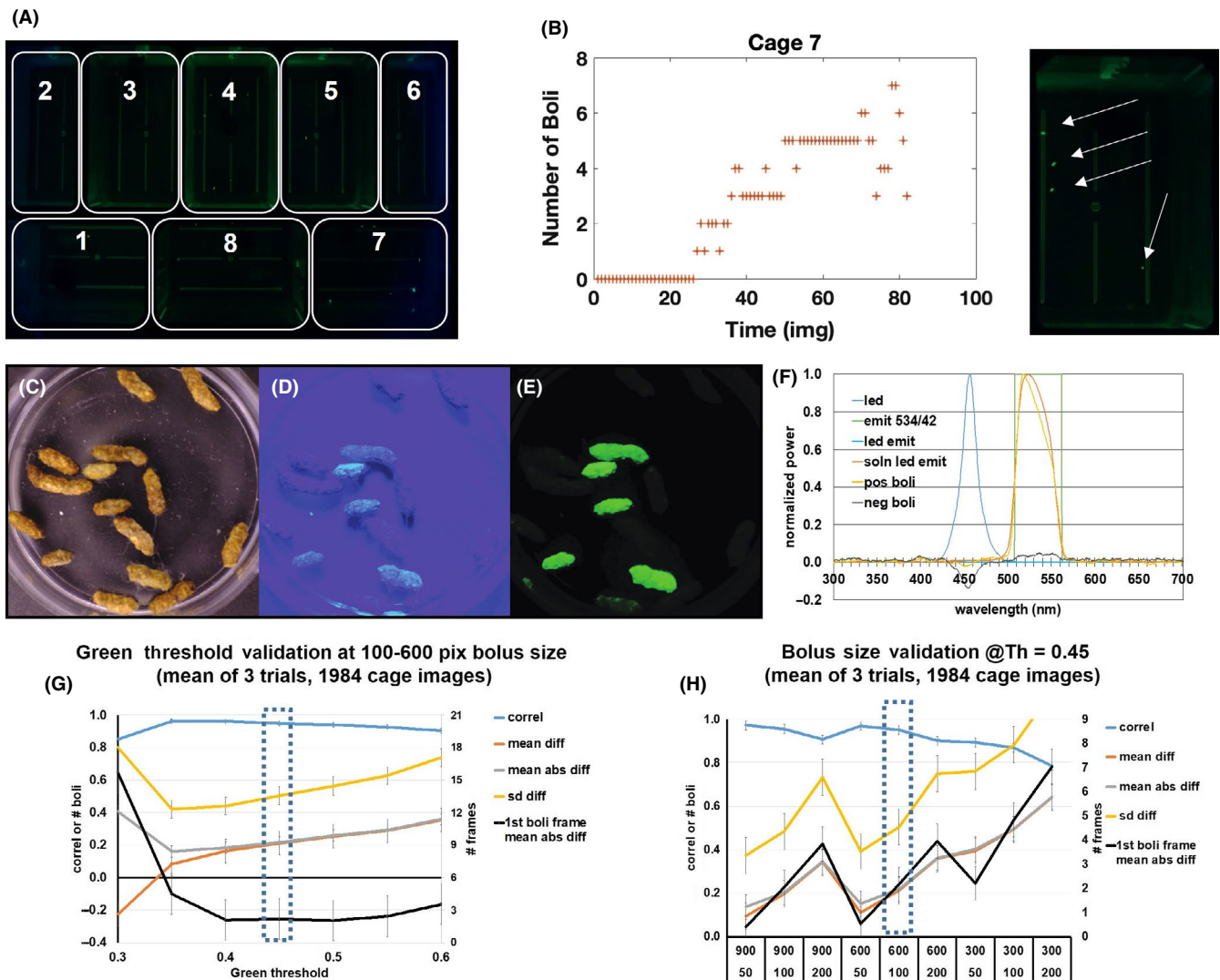


FIGURE 1 Fluorescent bolus imaging and automated scoring. A, Outline of the 8 imaged cages. B (left), Example of graph of number of boli counted in 1 of the 8 simultaneously imaged cages produced by automated MATLAB code. Reductions due to visual obstruction by mouse. (right): example of cage 4 with 4 fluorescent boli. C-E, Mixed fluorescent and control boli under white light (C), blue LED light (D), and emission filter (E). F, Spectra of LEDs (led), emission BP filter (emit), LED with emission filter (led emit), excitation of fluorescent solution (soln led emit), of positive boli (pos boli) and negative boli (neg boli). G, Validation of automated bolus counting vs manual of images' green layer brightness threshold. Mean of correlation (correl), bolus count difference (diff), and its standard deviation across cages (SD diff), count absolute difference (abs diff) and gut transit time 1st bolus frame absolute difference (1st boli frame) between human and MATLAB code. Bolus size range 100-600 pixels. H, Validation of automated bolus counting vs manual of bolus size range (top: max, bottom: min). Green threshold 0.45. Same validation parameters as G. Box in G and H indicates identical criteria (0.45 green threshold, 100-600 pixels bolus size range). Errors bars indicate SD

(Dell, P2415Qb) was connected to the camera to set optimal focus distance. An external intervalometer (JJC, TM Series) triggered the Sony to take 5-minute-spaced images, saved as jpg at minimal compression and highest resolution (6000 × 400 pixels, "fine", 7.3 MB per file). The camera was set to fully manual operation, ISO800, 4000K white balance, and other adjustments to neutral or default and 1/15th seconds exposure time (LEDs could be synchronized to this to reduce blue light expose, but were always on here). Each cage spanned between 1700 × 1100 pixels (cages 4 and 8; Figure 1A), 1700 × 800 pixels (cages 2 and 6), and 1500 × 1100 pixels (cages 1 and 7).

3.6 | Analysis

The images were analyzed post hoc for the presence of fluorescent boli, per cage, over time, by custom MATLAB code (Figure 2D). For each RGB jpg image, first, the size of the brightly fluorescing boli (100-600 pix) is identified in the green layer thresholded at 45% brightness, for each cage area (defined by their four corners). Subsequently, only those boli are counted that have a mean RGB 8-bit value of at least 0, 50, and 30, and no more than 50, 255, and 255, respectively, for the red, green, and blue layers. The analysis generates a figure with a graph per cage (Figure 1B) and exports the

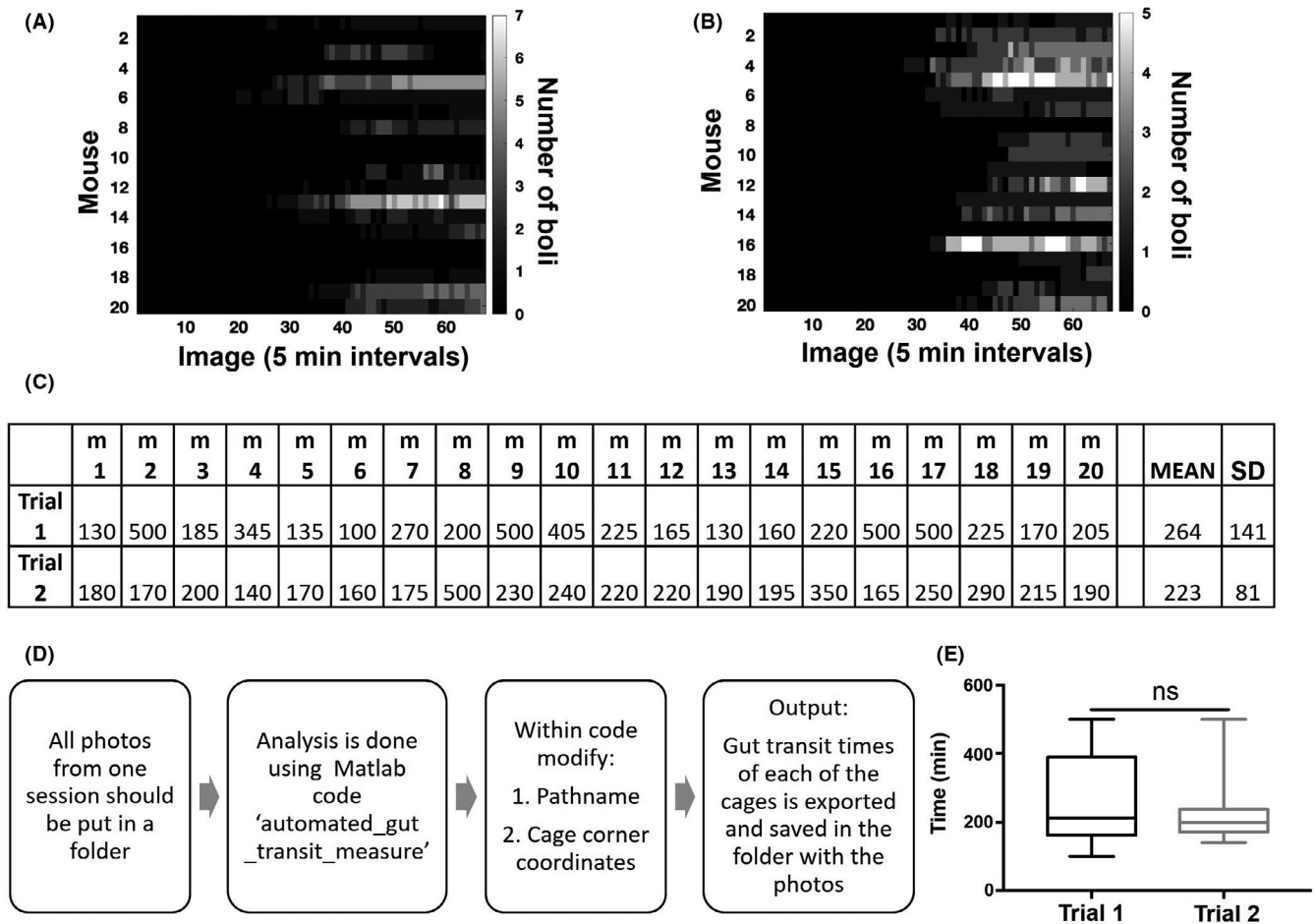


FIGURE 2 Automatically scored gut transit time and number of boli per cage. A-B, Number of fluorescent boli detected in each mouse cage (1-20) in the first trial (A) and retested a week later (B). C, Gut transit time, directly scored by MATLAB routine as the time after gavage of fluorescent powder suspension at which first fluorescent boli appeared. Mean and SD calculated by MATLAB. D, Flowchart detailing the procedure to perform the analysis. Note downloadable MATLAB code has extensive annotations to guide individual fine tuning. E, Box and whisker plot illustrating the difference in gut transit time over the two trials. Data represented as median and IQR. (data analyzed in GraphPad Prism. (n.s.: not significant)

transit time of each mouse. Variances are reported as standard deviations (SD).

4 | RESULTS

To accurately measure gut transit time, we utilized an automated imaging approach of eight mouse cages (Figure 1A) using a fluorescent powder as our marker of gut transit time. This provides excellent contrast of boli that do and do not include gavaged material. We can subsequently determine an accurate unbiased time of the first fecal boli. Figure 1B shows the result of the automated analysis for 1 mouse for 1 experiment across 81 frames (405 minutes). Fluorescent boli (from gavaged mice) are indistinguishable from control non-fluorescent boli (from an un-gavaged mouse) when lit by a common white fluorescent light tube (Figure 1C) and the LED-excitation filter assembly alone (Figure 1D). The addition of the emission filter placed before a camera (Figure 1E) demonstrates a clear differentiation of

the fluorescent boli, reducing any remaining background LED light, affording this approach its remarkable selectivity and sensitivity.

Analysis of the light spectrum (measured with ASEQ Instruments LR1) of the LED-excitation assembly peaks around 460 nm (Figure 1F); this is subsequently and appropriately rejected by the camera's band-pass emission filter. The emission spectrum of the powder suspension was similar to that of the fluorescent boli demonstrating that its transit and incorporation into boli did not affect its fluorescent emission. Negative boli (10 boli) only show very weak fluorescence (<5% of positive boli) under the same light and measurement conditions, providing a ~20-fold contrast ratio.

We examined the impact of different green image threshold and bolus size values on our algorithm in comparison with manual scoring by a trained observer for 24 cages (20 mice, 1984 total images). The variances (\pm SD) are all due to the different similarity measures between the 3 testing sessions. The correlation is based on the similarity between vectorized data of 648-680 measures (8 cages \times 81-85 images) per session. In one analysis,

the green threshold was varied from 0.3 to 0.6 (Figure 1G, x-axis) while fixing bolus size between 100 and 600 pixels. The algorithm was highly accurate as evidenced by a high correlation coefficient between manual and automated counting ($r = .85-.96$; Figure 1G, blue line). The mean difference between automated and manual scored gut transit time (first boli frame) varied between 2.04 and 15.7 (Figure 1G) frames. Likewise, we varied the bolus size from 50-200 minimum to 300-900 maximum pixels while fixing the green threshold at 0.45 (Figure 1H). These also yielded a high correlation coefficient ($r = .78-.97$; Figure 1H, blue line) and 0.4-7.1 frame range to identify the first boli. We found that the optimal parameters that yielded the highest correlation coefficient and first frame identification, while minimizing false-positive counts was 0.45, with a bolus size range of 100-600 (Figure 1G-H, dashed line boxes). These parameters yielded $r = .95 \pm .02$ and transit time difference of 2.2 ± 3.0 frames (11 minutes).

Figure 2A shows the number of boli detected across 20 mice and 67 consecutive images (335 minutes) during their first trial and Figure 2B for the second trial. Cages show no positive boli for frames 1-24 (120 minutes), after which many cages show a rise to 1-6 fluorescent boli. Reductions of this number are typically due to visual obstruction by the mouse (imaging cages from below would avoid this) or coprophagy. Transit times on day 1 did not predict those on day 2, as the 2D correlation between these matrices was $r = .367$, 0.45 SDS above 10 000-times randomly mouse-reshuffled matrices ($r = .315 \pm .117$).

Across 20 mice, the time of first fluorescent bolus detection, a direct measure of gut transit time, is shown in Figure 2C: 264 ± 141 minutes after gavage on trial 1, not significantly different from the second trial (223 ± 81 minutes; mean \pm SD, Figure 2E). There was no mouse-specific pattern between trials, as their correlation was -0.062 , 0.27 SDS below 10 000-times reshuffled vectors ($r = .001 \pm .232$). Sigmoidal curve fitting appeared to reduce the coefficient of variation and also provide further insight into gut motility kinetics.

(fluorescpoop_detect_allimages_8cages_12_17_19_sigmoidfit.m).

Supplementary files can be found for download at Datadryad: <https://doi.org/10.5061/dryad.8sf7m0chv> and are listed in Data S1.

5 | CONCLUSION

Gavaging rodents with fluorescent pigments allows imaging gut transit time and defecation temporal patterning with very high sensitivity. Imaging thereof provides an unambiguous record, while automated scoring thereof provides validated, rapid, and unbiased analysis.

ACKNOWLEDGMENTS

We appreciate the technical support of the John B. Pierce Shop. We thank Dr Doug Storace and Ankita Gumaste for helpful comments on the manuscript. We gratefully acknowledge support by NIH/NIDCD grants R01DC014723 and R01DC011286 and NSF grant IOS-1555880.

CONFLICT OF INTEREST

The authors declare no commercial interest in any of the described materials, their providers, or used methods.

AUTHOR CONTRIBUTIONS

KLB originated the study and wrote the manuscript. KLB and MI performed the experiments. KLB and JVV performed data analysis and created the figures. KLB, MI, RJ, and JVV edited and approved all the manuscript versions. RJ provided expert guidance to data interpretation and manuscript. JVV designed the fluorescent approach and created the MATLAB analysis.

ORCID

Justus V. Verhagen  <https://orcid.org/0000-0002-6090-0073>

REFERENCES

- Bassotti G, Antonelli E, Villanacci V, Salemme M, Coppola M, Annese V. Gastrointestinal motility disorders in inflammatory bowel diseases. *World J Gastroenterol*. 2014;20(1):37-44.
- Miller MS, Galligan JJ, Burks TF. Accurate measurement of intestinal transit in the rat. *J Pharmacol Meth*. 1981;6(3):211-217.
- Moore BA, Otterbein LE, Türlér A, Choi AMK, Bauer AJ. Inhaled carbon monoxide suppresses the development of postoperative ileus in the murine small intestine. *Gastroenterology*. 2003;124(2):377-391.
- Reed DE, Pigrau M, Lu J, Moayyedi P, Collins SM, Bercik P. Bead study: a novel method to measure gastrointestinal transit in mice. *Neurogastroenterol Motil*. 2014;26(11):1663-1668.
- Nagakura Y, Naitoh Y, Kamato T, Yamano M, Miyata K. Compounds possessing 5-HT₃ receptor antagonistic activity inhibit intestinal propulsion in mice. *Eur J Pharmacol*. 1996;311(1):67-72.
- Kashyap PC, Marcobal A, Ursell LK, et al. Complex interactions among diet, gastrointestinal transit, and gut microbiota in humanized mice. *Gastroenterology*. 2013;144(5):967-977.
- Li Z, Chalazonitis A, Huang Y-Y, et al. Essential roles of enteric neuronal serotonin in gastrointestinal motility and the development/survival of enteric dopaminergic neurons. *J Neurosci*. 2011;31(24):8998-9009.
- Kimball ES, Palmer JM, D'Andrea MR, Hornby PJ, Wade PR. Acute colitis induction by oil of mustard results in later development of an IBS-like accelerated upper GI transit in mice. *American Journal of Physiology-Gastrointestinal and Liver*. *Physiology*. 2005;288(6):G1266-G1273.
- Yang M, Fukui H, Eda H, et al. Involvement of gut microbiota in the association between gastrointestinal motility and 5HT expression/M2 macrophage abundance in the gastrointestinal tract. *Molecular medicine reports*. 2017;16(3):3482-3488.
- Welch MG, Margolis KG, Li Z, Gershon MD. Oxytocin regulates gastrointestinal motility, inflammation, macromolecular permeability, and mucosal maintenance in mice. *Am J Physiol Gastrointest Liver Physiol*. 2014;307(8):G848-G862.
- Coronas-Samano G, Baker KL, Tan WJT, Ivanova AV, Verhagen JV. Fus1 KO Mouse as a model of oxidative stress-mediated sporadic Alzheimer's disease: circadian disruption and long-term spatial and olfactory memory impairments. *frontiers in aging*. *Neuroscience*. 2016;8(268):1-26.
- Coronas-Samano G, Ivanova AV, Verhagen JV. The habituation/cross-habituation test revisited: guidance from sniffing and video tracking. *Neural Plast*. 2016;2016:14.
- Bohlen M, Hayes ER, Bohlen B, Bailoo JD, Crabbe JC, Wahlsten D. Experimenter effects on behavioral test scores of eight inbred

- mouse strains under the influence of ethanol. *Behav Brain Res.* 2014;272:46-54.
14. Neely C, Lane C, Torres J, Flinn J. The effect of gentle handling on depressive-like behavior in adult male mice: considerations for human and rodent interactions in the laboratory. *Behav Neurol.* 2018;2018:7.
 15. Sorge RE, Martin LJ, Isbester KA, et al. Olfactory exposure to males, including men, causes stress and related analgesia in rodents. *Nat Methods.* 2014;11(6):629-632.
 16. Bunnett NW. The stressed gut: contributions of intestinal stress peptides to inflammation and motility. *Proc Natl Acad Sci USA.* 2005;102(21):7409.
 17. Larauche M, Mulak A, Taché Y. Stress-related alterations of visceral sensation: animal models for irritable bowel syndrome study. *J Neurogastroenterol Motil.* 2011;17(3):213-234.
 18. Enck P, Merlin V, Erckenbrecht JF, Wienbeck M. Stress effects on gastrointestinal transit in the rat. *Gut.* 1989;30(4):455-459.

SUPPORTING INFORMATION

Additional supporting information may be found online in the Supporting Information section.

How to cite this article: Baker KL, Izydorczak M, Jackson R, Verhagen JV. An automated sensitive approach for measuring whole gut transit time. *Neurogastroenterology & Motility.* 2020;00:e13894. <https://doi.org/10.1111/nmo.13894>